Japanese Journal of Applied Physics

PROGRESS REVIEW • OPEN ACCESS

Lipid bilayer platforms for parallel ion channel recordings

To cite this article: Maurits R. R. de Planque 2022 *Jpn. J. Appl. Phys.* **61** SC0804

OPEN ACCESS

Japanese Journal of Applied Physics **61**, SC0804 (2022) **PROGRESS REVIEW**

https://doi.org/**10.35848/1347-4065/ac4f7a**

Lipid bilayer platforms for parallel ion channel recordings

Maurits R. R. de Planque

School of Electronics and Computer Science, University of Southampton, Southampton SO17 1BJ, United Kingdom

*E-mail: m.deplanque@soton.ac.uk

Received December 13, 2021; revised January 24, 2022; accepted January 26, 2022; published online March 30, 2022

The ion flow through channel proteins embedded in a lipid bilayer membrane can be recorded as an electrical current, enabling biophysical characterization and pharmacological drug screening at a single-channel level. These measurements are challenging because the self-assembled bilayers are fragile and the currents are in the pA–nA range. This concise review introduces the bilayer recording methodology, with an emphasis on the requirements for full electrophysiology assays. The self-assembled lipid bilayer, formed in a ~100 μm diameter aperture in between two aqueous chambers, is critical. Various approaches to increase the measurement throughput by scaling to aperture arrays are discussed in terms of current-amplifier technology, bilayer stability, ion channel incorporation, system functionality and obtained single-channel data. The various bilayer recording platforms all have advantages and limitations. Combining the strengths of the different platform architectures, for example, the use of shaped apertures, will be essential to realize and also automate parallel ion channel recordings. © 2022 The Author(s). Published on behalf of The Japan Society of Applied Physics by IOP Publishing Ltd

1. Introduction

Cell membrane-embedded proteins that act as ion channels or porins are functionally characterized by their ion flux, which is measured as an electrical current with the voltage-clamp technique.[1)] When it is not possible or not desirable to perform these measurements by sealing a glass nanopipette to the membrane of a biological cell, ion channels can be incorporated in an artificial membrane of synthetic or purified lipid molecules.[2)] Such model cell membranes, which self-assemble from lipids at the interface between two aqueous compartments, can be handled in most laboratories because they do not require cell culture and its associated infrastructure. The main systems are aperture-suspended, hydrogel-supported and droplet-interface lipid bilayers.[3,4)] For the latter two systems, access to one or both aqueous compartments is restricted, hence aperture-suspended lipid bilayers are the most versatile in terms of applications, including ion channel drug screening and nanopore sensing.

As shown in Fig. 1, two aqueous compartments, each with an Ag/AgCl electrode connected to an amplifier, are separated by a septum with an aperture. When lipid dissolved in a volatile solvent such as chloroform is added, a lipid monolayer forms at the water–air interface. By raising and lowering the water level, this interface moves over the aperture and a lipid bilayer can form inside the aperture. The aperture should be pre-coated with a non-volatile solvent such as hexadecane to facilitate lipid contact with the aperture wall. The septum has to be hydrophobic so that excess solvent can drain away and it should be of sufficient thickness to exhibit a negligible capacitance (low pF), enabling high-bandwidth (≥10 kHz) and low-noise (<1 pA) current measurements.[5,6)] Teflon films of 20–50 μm thickness are widely used, also because this thickness range imparts mechanical robustness. The septum aperture is critical for bilayer formation and stability.

In the planar lipid bilayer structure, the hydrophobic hydrocarbon chains of lipid molecules are in contact with each other to avoid contact with water. As there are no covalent bonds between lipids and the bilayer is only ~5 nm thick, it is no surprise that aperture-suspended bilayers are inherently fragile. They can be difficult to form and current measurements of channels or pores necessitate applying a potential over the bilayer, which has a destabilizing effect. Apertures should at most be ~200 μm in diameter and the highest potential that can be applied is ~200 mV. Smaller bilayers are more stable but below a diameter of ~30–50 μm vesicle fusion, which is used to incorporate ion channels into the bilayer, becomes problematic.[7–9)] It has been demonstrated that shaped apertures, where the septum wall tapers down to 0.2–2 μm thickness (Fig. 2), give more stable bilayers than cylindrical apertures.[7,8)] It is thought that the reduced septum thickness at the narrowest point of a shaped aperture provides a defined anchor point for the suspended bilayer, preventing substantial bilayer movement along the aperture wall after formation.

2. Experimental requirements

For most applications, once formed, aperture-suspended bilayers have to withstand perturbations of the electrolyte solution, including lowering and raising the water–air interface over the aperture. The composition of the solution may have to be changed and mixing has to occur, for example to facilitate vesicle fusion or to gradually increase the concentration of a drug to establish the dose-response relationship for an ion channel receptor. Changes to the applied potential are also important to characterize ion channels. With the standard ionic strength of ~150 mM, potentials of 100–120 mV are preferred so that single-channel currents can reach ~10 pA. Detailed protocols are available in the literature.[10)]

When nanopores, which have a wider channel, are used as sensors,[11,12)] the preferred salt concentration is 1 M so that analyte interactions with the pore result in larger channel current changes (Fig. 3). For microRNA quantification, using different salt concentrations in the two compartments increases the electrophoretic driving force towards the pore. This improves the limit of detection, but steep salt gradients

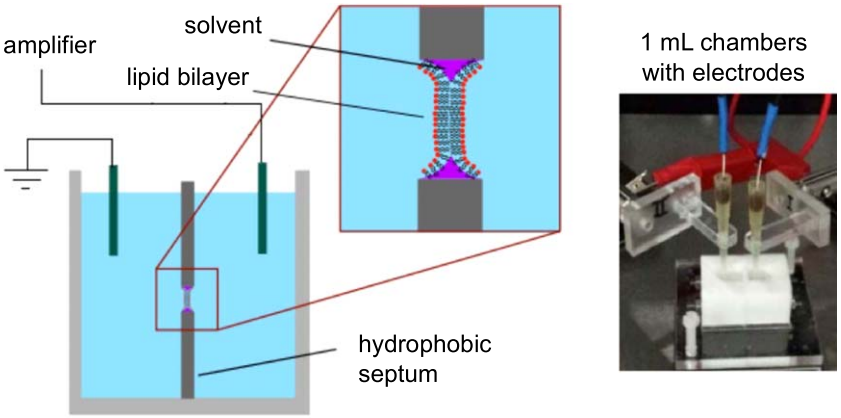

Fig. 1. (Color online) Conventional current recording setup for ion channels or nanopores embedded in a lipid bilayer which is suspended in an aperture in a hydrophobic septum that is clamped between two aqueous chambers, each with an Ag/AgCl electrode connected to a voltage-clamp amplifier.

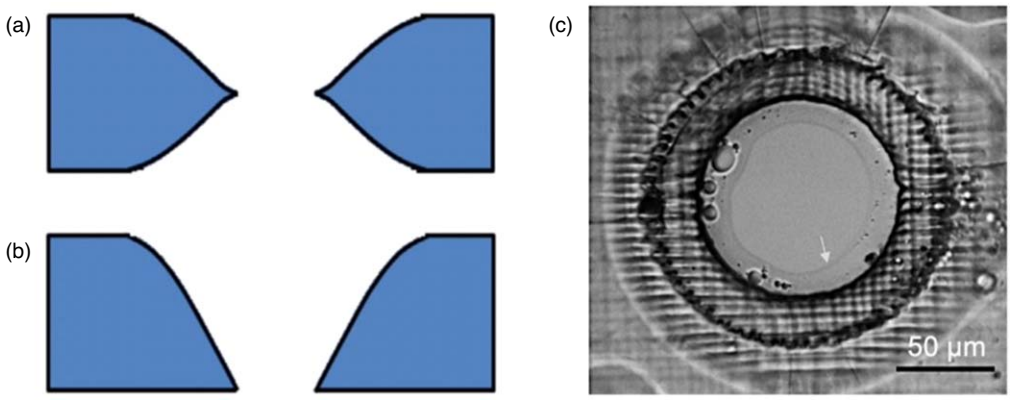

Fig. 2. (Color online) (a), (b) Shaped aperture geometries of ~80 μm inner diameter and 50 μm septum thickness. (c) Optical microscopy image of a bilayer suspended in a lithographically defined shaped aperture. The arrow indicates the solvent annulus which connects the bilayer to the aperture edge. Reprinted with permission from Ref. 7. Copyright 2014 Elsevier.

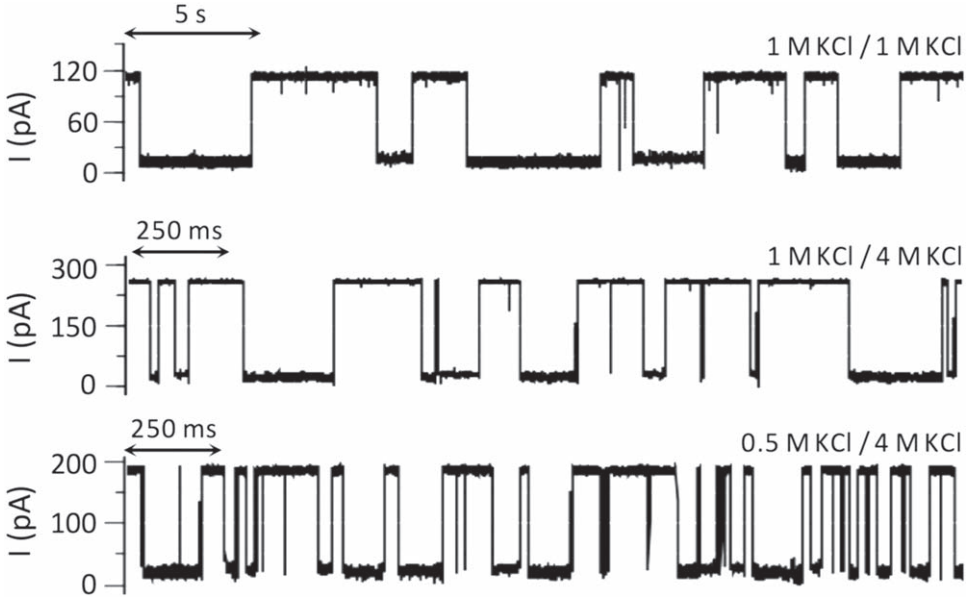

Fig. 3. Current–time traces for symmetrical 1 M KCl and for 1/4 and 0.5/4 M *cis*/*trans* KCl gradients, recorded at +120 mV. Each transient current decrease event represents a single microRNA molecule traversing an α-hemolysin nanopore. Salt gradients increase event frequency and reduce translocation times. Reprinted with permission from Ref. 13. Copyright 2017 American Chemical Society.

(e.g. 20-fold: 0.2 M/4 M KCl) destabilize the bilayer,[13] also when lithographically defined shaped apertures are used.[7]

Manual experiments with a single lipid bilayer are time consuming and low throughput, mainly due to the difficulty of forming and maintaining aperture-suspended bilayers. More routine application of ion channel or nanopore recordings with the lipid bilayer technique necessitates higher experimental throughput. First and foremost, this requires

optimization of bilayer stability under typical assay conditions, e.g. perturbation of the aqueous chambers and vesicle fusion for ion channel incorporation. In addition, platform architectures for parallel recordings would present a major advance, especially in combination with automated bilayer formation. This requires multiple pairs of aqueous chambers, each with its own electrodes and connected to an individual voltage-clamp amplifier. The complete system should enable sub-pA measurements at a bandwidth of $\geqslant$10 kHz.[5)]

3. Voltage-clamp current amplifiers

Ion channel recordings with lipid bilayers are typically only performed in research laboratories, mostly using research-grade patch-clamp amplifiers such as the Axopatch 200B or the HEKA EPC 10 instruments. These are designed for both patch clamping of cell membranes and for single-channel recordings with lipid bilayers, two different scenarios in terms of current amplitude and signal-to-noise requirements which necessitate different electronics.[6)] These instruments, priced around $10 k, control a single set of electrodes (i.e. are single-channel) and can achieve sub-pA noise levels for bilayer recordings at 10 kHz bandwidth. An example of a complete measurement system is shown in Fig. 4. In a typical voltage-clamp experiment, the operator sets a potential at which the membrane or bilayer should be maintained, e.g. +100 mV. The actual electrochemical potential is measured and any deviation from the "command" potential is continuously compensated by current injection. This represents the ion current flowing through the membrane's ion channels at the specified potential.[1,14)]

Interestingly, an open-source amplifier for bilayer recordings, implemented on a printed circuit board, has recently been published.[15)] Its design can be contrasted with the detailed construction description of a basic patch-clamp amplifier, primarily intended for educational purposes, for ion channel current measurements from pipette-patched cells.[14)] Because aperture-suspended bilayers have negligible leakage currents and low access resistance and are not contacted by glass pipettes,[15)] voltage-clamp amplifiers for bilayer recordings do not need circuits for series resistance compensation, pipette capacitance compensation, adjustment of pipette offset potentials or leak substraction.[1,14)]

Two-channel or four-channel versions of the commercial amplifiers, which are essentially full copies of the corresponding single-channel system, are also available. Because patch clamping of cell membranes has been successfully automated with the planar patch clamp technique, where cells are sucked onto apertures in a chip and ion channel currents from tens to hundreds of cells can be measured simultaneously,[16)] various multi-channel amplifiers can be purchased as well. These include the 4 to 16-channel Triton, the 8 to 96-channel Flex, the 16 to 128-channel Jet and the 48 to 384-channel Apollo amplifiers from Tecella. However, it is likely that the instruments with more channels are optimized for nA currents from multiple ion channels in a membrane patch.

An alternative approach is the design of application specific integrated circuits (ASICs) that function as miniaturized amplifiers, with electronic components defined as an integrated circuit on a chip manufactured in a complementary metal-oxide-semiconductor (CMOS) foundry.[6,17)] It is advantageous that these miniaturized amplifiers can be positioned in close proximity to the lipid bilayer, reducing membrane-amplifier interconnect (e.g. electrode wiring) capacitance and negating the requirement for a pre-amplification headstage.[17,18)] Several academic groups have designed ASIC current amplifiers for bilayer recordings; some of these are now used in commercial instruments.[18–22)] ASIC amplifiers for cellular recordings have also been described.[23–25)] The prime example of commercial applications of ASIC amplifiers is the MinION DNA sequencer from Oxford Nanopore Technologies. With a footprint of 10×2 cm, it consists of 512 amplifiers, on top of which a disposable flow cell is positioned which contains 2048 scaffolded nanopores for parallel DNA or RNA sequencing.[26)]

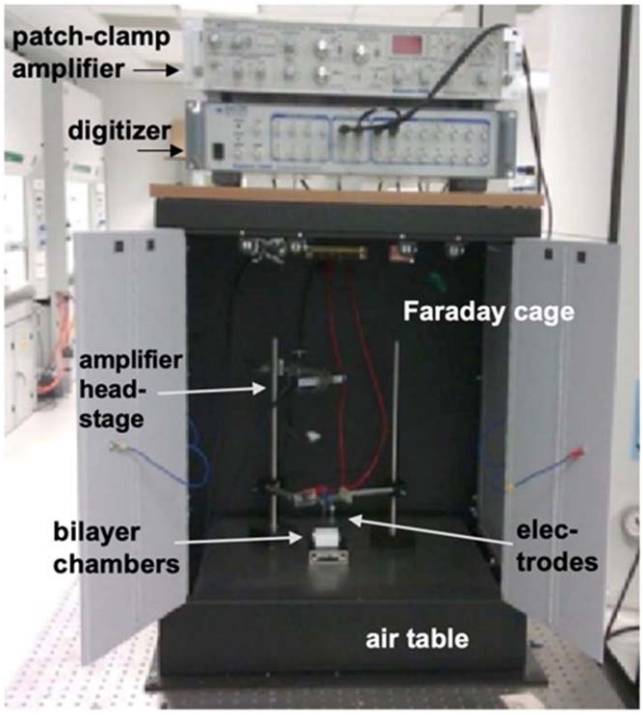

Fig. 4. (Color online) A standard system for the recording of pA-range currents of ion channels in an aperture-suspended lipid bilayer consists of a commercial patch clamp amplifier, connected to Ag/AgCl electrodes in the bilayer-flanking aqueous compartments through a digitizer and a headstage for current-to-voltage conversion and signal pre-amplification. The Faraday cage, which does not have to be much larger than the bilayer chambers and electrode holders, is essential while an anti-vibration platform is recommended.

4. Parallel platforms

For high-throughput recordings of ion channels or nanopores, an intuitive approach is to multiply the classical setup with two fully accessible aqueous compartments on either side of a vertical aperture-suspended bilayer (Fig. 1). Ahmed et al. presented the concept of a 96-bilayer tray with 8 rows of 8 sets of 3D-printed aqueous chambers of $\sim$40 μl volume [Figs. 5(a)–5(c)].[27,30)] They described clamping of aperture chips in between a row of four opposite chambers and demonstrated recordings for a single bilayer with the four-bilayer row positioned in a Faraday cage. OmpF porin was added as a micellar solution and self-insertion into the bilayer was facilitated by raising and lowering the aqueous solution of 1 M NaCl with a pipettor. At $-$100 mV potential, the rms current noise was 2.8–3.4 pA at 10 kHz bandwidth.[27,30)]

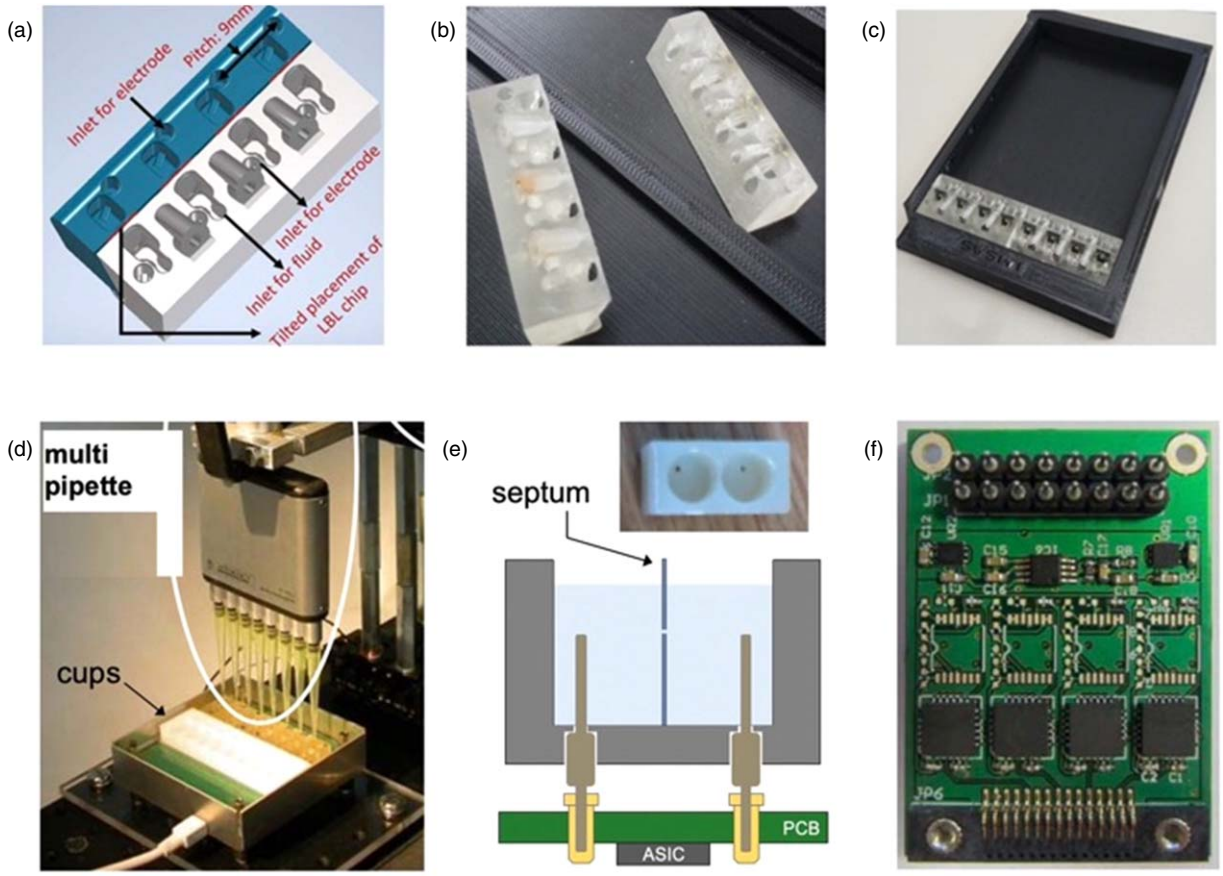

Fig. 5. (Color online) Bilayer arrays with fully accessible aqueous compartments. (a) Design for chamber arrays with an aperture chip clamped in between four chamber pairs, (b) a 3D-printed prototype for four bilayers, and (c) a 3D-printed prototype for 8 bilayers in a tray with a capacity for 8 of such rows.[27)] (d) A linear array of 8 bilayer cups on a printed circuit board with 8 ASIC current amplifiers, depicted with a computer-controlled 8-channel pipette.[28)] Panel is adapted (CC BY 4.0 license) from the original publication. (e) Cross-sectional diagram showing two aqueous chambers separated by a septum with an aperture for bilayer formation, with electrode pins connecting to an ASIC amplifier, and a photo of a bilayer cup block with pin openings. (f) Underside of a printed circuit board with four ASIC amplifiers in a 2×4 array design. © 2015 IEEE. Reprinted with permission from Ref. 29.

Parallel recordings would have required the use of a multi-channel amplifier and a design approach for wiring and inserting 96 working and reference electrodes from above into the fluid reservoirs.

An alternative design is to position ASIC amplifiers under each set of aqueous chambers, with electrodes inserted from the bottom of the aqueous reservoirs [Figs. 5(d)–5(f)]. Thei et al. demonstrated a printed circuit board (PCB) with a 4×3 array of disposable bilayer chambers on the top side and an equivalent array of ASICs on the bottom, which is placed in a metal box acting as a Faraday cage.[19)] Each bilayer chamber consists of a polymer block ($9 \times 18 \times 10$ mm, $W \times L \times H$) with two cylindrical cavities of 150 μl volume separated by a $\sim$50 μm thick septum containing a microdrilled aperture of 200 μm diameter. Transient blocking of the α-hemolysin (αHL) nanopore by the β-cyclodextrin molecule was shown for three bilayers simultaneously. These parallel current recordings were obtained at bandwidths between 0.5 and 4 kHz, in 1 M KCl solution at 60 mV potential. A modified design with a single row of 8 bilayer chambers, optimized for fluid manipulation with a computer-controlled 8-channel pipette [Fig. 5(d)], enabled automated formation of six bilayers in parallel, and αHL recordings in two bilayers simultaneously were also shown.[28,31)]

The feasibility of parallel recording depends on the ease of formation of aperture-suspended bilayers and of their stability under experimental conditions. Microdrilled apertures of 150–250 μm diameter, as in the classic bilayer cup design of Warner Instruments, give unstable bilayers because of the relatively large diameter, edge roughness and cylindrical geometry.[7)] With the platform of Thei et al. it was not possible to maintain 12 bilayers at the same time, and perturbations of the aqueous chambers to promote ion channel incorporation destabilize the remaining bilayers. This is a significant concern because reformation of a bilayer, or additional manipulations to control incorporation, requires opening the Faraday cage, which disrupts the recordings from all bilayers in the array. Hence any array platform for simultaneous electrical recordings requires an aperture geometry that maximizes the stability of suspended bilayers. Shaped apertures of 20–30 μm diameter with nanometer scale tapering at the aperture edge and outwards micrometer scale tapering [Fig. 6(a)], enable extremely stable aperture-suspended bilayers, as quantified by aspiration cycles, centrifugal force, large changes to the applied potential and by bilayer lifetime.[9)]

Recently, a 4×4 array of shaped apertures was reported by Miyata et al.[32)] As illustrated in Fig. 6, a vertically oriented holder for 16 aperture chips was initially flanked by two aqueous compartments of 1.4 ml volume. Bilayer formation was achieved row-by-row by raising the lipid monolayer-covered buffer solution over all the sixteen 40 μm

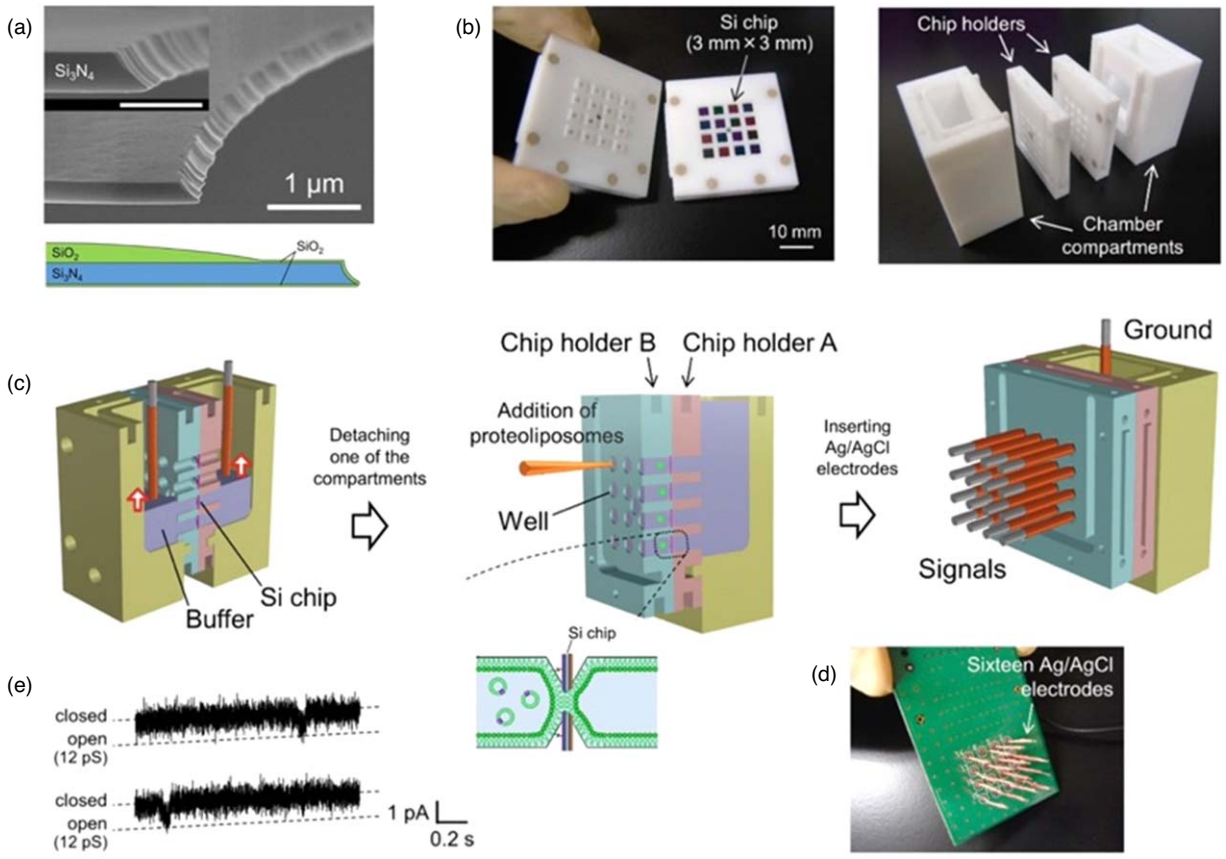

Fig. 6. (Color online) Shaped-aperture array for a conventional multichannel amplifier. (a) Scanning electron microscopy image and diagram of shaped aperture with nanoscale tapering at the edge and microscale tapering towards the edge.[9] (b) Two-part chip holder with 16 shaped-aperture chips (left) and with shared-chamber compartments (right).[32] (c) Schematic drawings of array formation, from bilayer formation to removing one shared compartment, injecting proteoliposomes in individual chip wells and closing these wells with an electrode holder.[32] (d) Photograph of 16-electrode array.[32] (e) Example of hERG channel current recordings in one of the bilayers of the array.[32] The panels are adapted (CC BY 4.0) from the original publications.[9,32]

diameter apertures. Subsequently, one compartment was detached, exposing the ∼40 μl wells on the *cis* side of each bilayer and 3 μl of proteoliposome solution was added to each well. These microwells were then capped, and isolated from each other, by the attachment of an electrode holder which positioned a horizontally oriented active electrode in each well (Fig. 6). Current recordings of the 16 bilayers were obtained with a 16-channel patch clamp amplifier, with a vertical common ground electrode in the shared *trans* compartment.[32] Despite the associated mechanical and electrical perturbations, 13 bilayers were formed on average. Miyata et al. typically observed hERG ion channel activity, in 120 mM KCl at −100 mV, in six bilayers simultaneously.[32] Proteoliposome fusion is more demanding than using self-inserting ion channels but fusion can be facilitated, for example by centrifugation at ∼40 × g.[33]

5. Alternative bilayer array formats

Although lipid bilayer systems with fully accessible buffer compartments are the most versatile in terms of applications, bilayers of several other systems are inherently more stable because of a smaller surface area and/or access to a reservoir of lipid-containing solvent.[3,4]

Several groups have used lithographically defined microcavities of ∼10 μm depth and ∼30 μm diameter with a horizontal lipid bilayer "painted" from a solvent-lipid mixture on top (Fig. 7).[18,29,34] These contain a microscale electrode at the bottom of the cavity,[35] while the other electrode is immersed in the upper reservoir of ∼0.5 ml volume. Baaken et al. demonstrated a 4 × 4 microcavity array with a shared aqueous chamber [Fig. 7(a)] and 16 micro-electrodes connected to a commercial 16-channel patch clamp amplifier.[34] All 16 bilayers were readily formed and maintained. The addition of the self-inserting αHL nanopore resulted in single-channel incorporation in 5 bilayers on average, with other bilayers having no or two nanopores [Fig. 7(b)]. Single-molecule analysis of poly(ethylene glycol) in the pore, in 1–4 M KCl, at +40 mV potential and 20 kHz bandwidth, were possible but additional analysis was required to correct for the slow frequency response time of the multichannel amplifier.[34] For a single microcavity-supported bilayer with an ASIC amplifier underneath [Figs. 7(c), 7(d)], Hartel et al. incorporated the ryanodine receptor protein RyR1 by proteoliposome fusion and could resolve calcium-induced channel gating events, in 1 M KCl at −200 mV, as short as 2–3 μs at 500 kHz bandwidth [Fig. 7(e)].[18] At frequencies >10 kHz, the performance of the ASIC amplifier exceeds that of the benchmark Axopatch 200B instrument in terms of current noise.[6,18]

The lipid bilayer formed at the contact area of two aqueous droplets inside a lipid-containing solvent solution [Fig. 8(a)] is extremely stable.[3] Kawano et al. developed an array of 16 microwell pairs, each of ∼40 μl volume and separated by a contact area-defining septum, in a double-row layout suitable for an 8-channel multipipette (Fig. 8), enabling automated bilayer formation by subsequent injection of a ∼10 μl

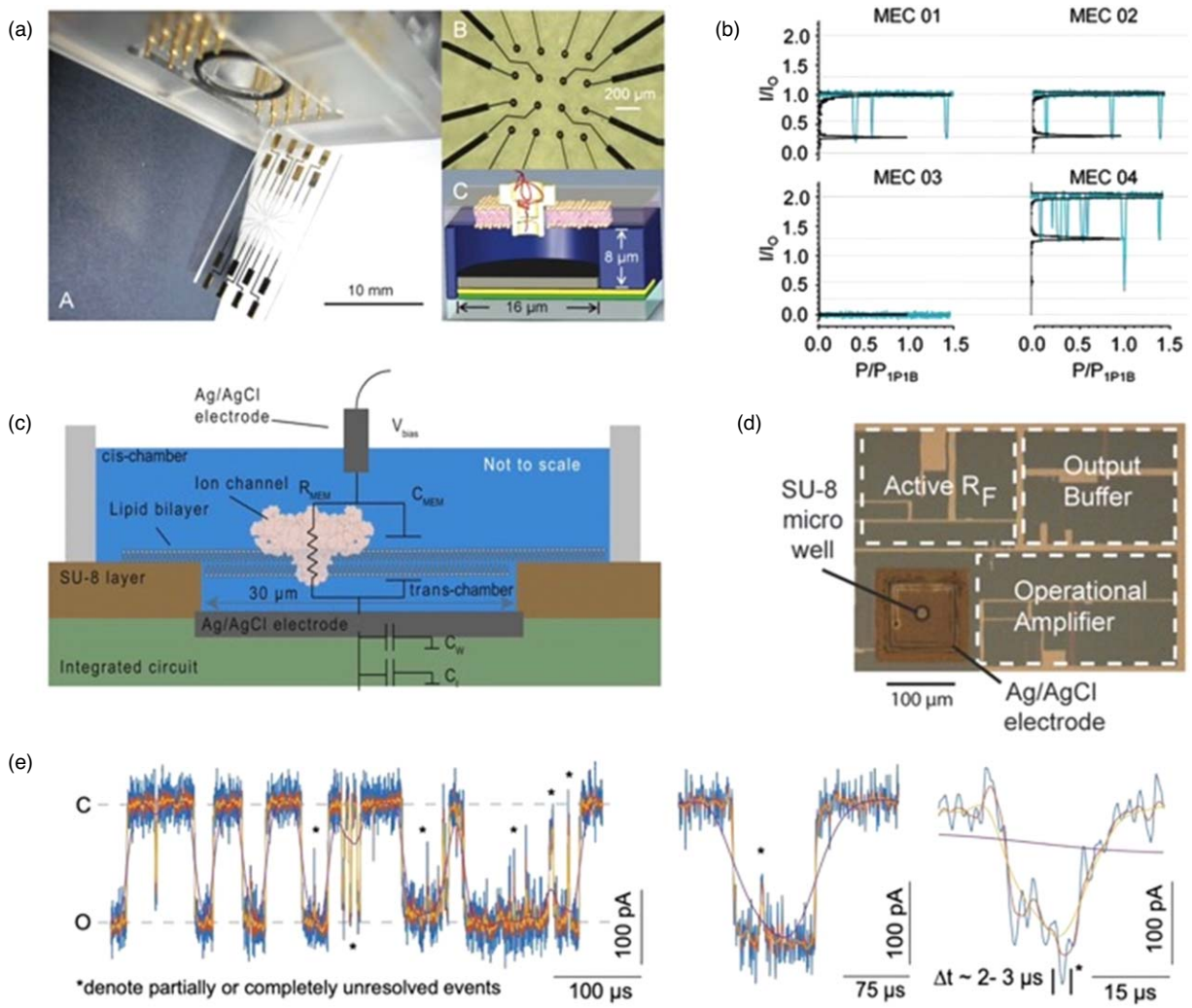

Fig. 7. (Color online) Horizontally suspended lipid bilayers without access to the bottom compartment. (a) Chip holder for the multielectrode cavity array with the corresponding chip prior to insertion (panel A), with magnified view of the 4 × 4 microcavity array and gold electrode tracks (panel B), and a schematic diagram (panel C) of a microcavity defined in SU8 resist (dark blue) on gold (yellow) on chrome (green) on a glass substrate (transparent light gray), including an Ag/AgCl electrode (dark gray and black) at the bottom of the cavity. (b) Representative histograms (black) and overlaid current traces (cyan) of parallel recordings for four bilayers, showing polymer-mediated blockages of α-hemolysin pores, with the normalized current corresponding to the number of inserted pores. Reprinted (a) and adapted (b) with permission from Ref. 34. Copyright 2011 American Chemical Society. (c) Schematic diagram of SU8-defined microwell on top of ASIC amplifier: the lower Ag/AgCl reference electrode pellet directly connects to the ASIC transimpedance amplifier while a conventional Ag/AgCl wire in the top reservoir acts as the active electrode. A lipid bilayer spans the microwell opening and separates it from the upper reservoir. Adapted with permission from Ref. 6. Copyright 2019 Elsevier. (d) Microscopy image of ASIC amplifier chip with SU8 microwell. Reprinted with permission from Ref. 21. Copyright 2013 American Chemical Society. (e) ASIC microwell current recording of a ryanodine receptor RyR1 ion channel gating at four different bandwidths, 10 kHz (purple), 100 kHz (yellow), 250 kHz (red), and 500 kHz (blue), illustrating the gating events that are not fully resolved at 10 kHz bandwidth.[18)]

lipid-containing decane droplet and a ~20 μl channel-containing buffer droplet.[36)] Parallel recordings were performed with a commercial 16-channel patch clamp amplifier at 5 kHz bandwidth and were 1 kHz low-pass filtered. A large amount of data was obtained, on self-inserting as well on proteoliposome-delivered ion channels, in 1 M KCl for alamethicin and αHL and in 130 or 140 mM KCl solution for two different potassium channels, at potentials ranging from −150 to +150 mV. Moreover, by manual injection of increasing amounts of potassium channel blockers, channel inhibition by verapamil and iberiotoxin was quantified.[36)] The same research group later demonstrated a platform with a sophisticated electronics interface, including disposable microwells that click onto electrode pins [Fig. 8(f)], on which drug interactions with various membrane proteins, incorporated in the interdroplet bilayer by fusing of cell membrane fractions, were studied.[37)]

6. Overview

The conventional bilayer setup of an aperture-suspended lipid bilayer in between two aqueous compartments (Figs. 1 and 4) gives maximal flexibility because the solution composition can be changed throughout the assay, but measurements are laborious and low-throughput. The engineering challenge is how to scale this to automated multi-bilayer platforms. A critical requirement is that arrayed bilayers should be of maximum stability, to prevent frequent bilayer reformation, which involves opening the Faraday cage and consequently disruption of the current recordings of the intact bilayers. Shaped apertures give the most stable suspended bilayers,[7,8)]

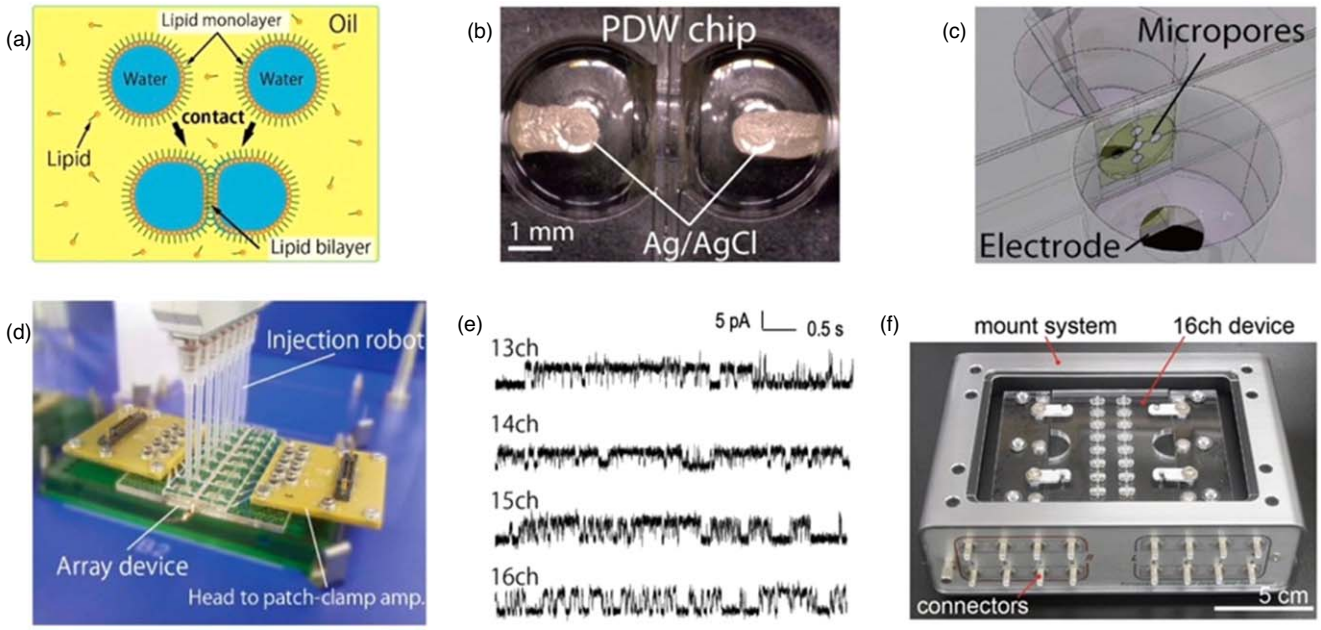

Fig. 8. (Color online) Interdroplet bilayer arrays. (a) Aqueous droplets in a lipid-solvent phase are covered by a lipid monolayer and bilayers form at droplet-droplet contact points.[36] (b) Two microdrilled chambers, with a parylene septum clamped in between, each with an Ag/AgCl electrode track at the bottom.[36] An aqueous droplet fills about half of the chamber and rests on the electrode. (c) The contact area between droplets is restricted to five apertures of 100 or 150 μm diameter, preventing the formation of larger bilayers and the associated increase in bilayer capacitance.[36] (d) A 2 × 8 double-well array for interdroplet bilayers with electrode tracks towards a 16-channel patch clamp amplifier.[36] Automated bilayer formation was achieved by subsequent injection of solvent-oil and ion channel-containing buffer droplets in each well. (e) Examples of parallel recordings of the hBK channel in four different interdroplet bilayers.[36] The panel is adapted (CC BY-NC-ND 3.0) from the original publication.[36] (f) The modified platform consists of a disposable acrylic layer with microwells that clicks onto an instrument mount with electrode pins leading to connectors for a multichannel amplifier.[37]

and the 16-bilayer array from Miyata et al. (Fig. 6) did indeed increase experimental throughput, achieving parallel recordings of the hERG ion channel in six bilayers.[32]

It would be interesting to implement the earlier proposals for array architectures,[19,30] i.e. multiple independent bilayer wells next to each other (Fig. 5), with a shaped aperture in between the two reservoirs. Such a design is compatible with pipettor robots while ASIC amplifiers can be positioned directly under the wells.[19,28,31] Manual pipetting is performed as gently as possible to avoid disrupting an aperture-suspended bilayer or to complicate its formation. In the bilayer cup design of Rossi et al., each aqueous chamber has a partial vertical partition which protects the aperture-suspended bilayer from direct contact with the fluid ejected from the automatic pipette.[28] Robotic formation of droplet-in-oil bilayer arrays has been achieved,[36,38,39] but the use of pipettor/dispenser robots for aperture-suspended bilayer systems remains to be systematically explored.

It has been shown that the integrated-circuit amplifiers specifically designed for current recordings from bilayers rather than cells, when placed in close proximity to the suspended bilayer, can rival or surpass the performance of bulky and costly commercial amplifiers designed primarily for cellular patch clamp.[6,34] This is especially important for bilayer arrays, negating the need for commercial multi-channel patch clamp amplifiers. ASIC amplifiers are now commercially available. The founders of the company Elements srl were associated with the bilayer array platforms of Thei et al. [Figs. 5(d)–5(f)].[19,31] The microcavity array platform of Baaken et al. has also been commercialized,[34] with the disposable microcavity array chips and the recording instrumentation supplied by the companies Ionera and Nanion Technologies, respectively. Bilayer formation on the microcavity array is essentially automated, with the lipid-in-solvent "painting" solution in the shared top reservoir spread out by a small stirrer bar until all 16 bilayers have formed.

Both the microcavity-suspended horizontal bilayer and the vertical interdroplet bilayer systems have limitations. The microcavity compartments are inaccessible after bilayer formation and arrays have a common top reservoir, while the droplets have limited accessibility and diffusion of molecules into the bulk solvent phase is unknown. However, their robust bilayers have enabled higher-throughput ion channel and nanopore recordings, with several publications presenting array data that would have been substantially more cumbersome to acquire with a traditional single-bilayer system.[34,36,37]

7. Conclusions

High-throughput automated ion channel recordings already exist in the form of cellular planar patch clamp, which has the significant advantages that ion channels are already present in the cell membrane, that cells can readily be suction-adsorbed on ~2 μm diameter apertures, and that the membrane contains many copies of the overexpressed ion channel of interest, implying that the measured currents are in the nA range.[16] However, for single-channel studies and the investigation of reconstituted (intracellular) membrane proteins, the lipid bilayer technique is preferred. The advances in parallel bilayer recording platforms, as outlined in this concise progress review, are promising. The achievement of

simultaneous ion channel recordings, even if not in all the bilayers of the array, do provide the motivation to pursue their further development.

Ideally, such platforms should consist of an array of independent lipid bilayers, each connected to its own high-bandwidth ASIC amplifier, positioned in an easily opened Faraday enclosure. The aqueous compartments flanking the bilayers should be fully accessible so that all solution changes (e.g. drug injection and subsequent mixing) can be performed at all assay stages. Substantial arrays need to be automated with a pipettor robot, capable of accessing individual bilayer chambers. Full automation necessitates an array management system which analyses current traces for each bilayer and decides when manipulation, such as bilayer reformation or solution change, is necessary at which array site. For the incorporation and subsequent functional characterization of the pharmacologically important ion channels, a remaining challenge is then to control the efficiency of proteoliposome fusion with the lipid bilayer.

Acknowledgments

The author thanks the organizers of the 2021 International Conference on Solid State Devices and Materials (SSDM2021) for the invited contribution,[40] on which this progress review is based in part.

ORCID iDs

Maurits R. R. de Planque https://orcid.org/0000-0002-8787-0513

1) A. Molleman, *Patch Clamping: An Introductory Guide to Patch Clamp Electrophysiology* (Wiley, Chichester, 2003).
2) C. Miller (ed.) *Ion Channel Reconstitution* (Springer, Boston, MA, 2013).
3) M. Zagnoni, Lab Chip **12**, 1026 (2012).
4) A. Hirano-Iwata, Y. Ishinari, H. Yamamoto, and M. Niwano, Chem. Asian J. **10**, 1266 (2015).
5) M. Mayer, J. K. Kriebel, M. T. Tosteson, and G. M. Whitesides, Biophys. J. **85**, 2684 (2003).
6) A. J. W. Hartel, S. Shekar, P. Ong, I. Schroeder, G. Thiel, and K. L. Shepard, Anal. Chim. Acta **1061**, 13 (2019).
7) S. Kalsi, A. M. Powl, B. A. Wallace, H. Morgan, and M. R. R. de Planque, Biophys. J. **106**, 1650 (2014).
8) A. Hirano-Iwata, K. Aoto, A. Oshima, T. Taira, R. Yamaguchi, Y. Kimura, and M. Niwano, Langmuir **26**, 1949 (2010).
9) D. Tadaki et al., Sci. Rep. **7**, 17736 (2017).
10) E. Zakharian, Methods Mol. Biol. **998**, 109 (2013).
11) W. Shi, A. K. Friedman, and L. A. Baker, Anal. Chem. **89**, 157 (2017).
12) J. W. F. Robertson, M. L. Ghimire, and J. E. Reiner, Biochim. Biophys. Acta Biomembr. **1863**, 183644 (2021).
13) J. Ivica, P. T. F. Williamson, and M. R. R. de Planque, Anal. Chem. **89**, 8822 (2017).
14) A. Rouzrokh, S. A. Ebrahimi, and M. Mahmoudian, Adv. Physiol. Educ. **33**, 121 (2009).
15) V. Shlyonsky and D. Gall, Pfluegers Arch. **471**, 1467 (2019).
16) D. C. Bell and M. L. Dallas, Br. J. Pharmacol. **175**, 2312 (2018).
17) M. Crescentini, M. Bennati, M. Carminati, and M. Tartagni, IEEE Trans. Biomed. Circuits Syst. **8**, 278 (2014).
18) A. J. W. Hartel, P. Ong, I. Schroeder, M. H. Giese, S. Shekar, O. B. Clarke, R. Zalk, A. R. Marks, W. A. Hendrickson, and K. L. Shepard, Proc. Natl. Acad. Sci. U. S. A. **115**, E1789 (2018).
19) F. Thei, M. Rossi, M. Bennati, M. Crescentini, F. Lodesani, H. Morgan, and M. Tartagni, IEEE Trans. Nanotechnol. **9**, 295 (2010).
20) B. Goldstein, D. Kim, J. Xu, T. K. Vanderlick, and E. Culurciello, IEEE Trans. Biomed. Circuits Syst. **6**, 111 (2012).
21) J. K. Rosenstein, S. Ramakrishnan, J. Roseman, and K. L. Shepard, Nano Lett. **13**, 2682 (2013).
22) M. Amayreh, G. Baaken, J. C. Behrends, and Y. Manoli, IEEE Trans. Biomed. Circuits Syst. **13**, 225 (2019).
23) P. Weerakoon, E. Culurciello, Y. Yang, J. Santos-Sacchi, P. J. Kindlmann, and F. J. Sigworth, J. Neurosci. Methods **192**, 187 (2010).
24) F. Laiwalla, K. G. Klemic, F. J. Sigworth, and E. Culurciello, IEEE Trans. Circuits Syst. I Regul. Pap. **53**, 2364 (2006).
25) S. Shekar, K. Jayant, M. A. Rabadan, R. Tomer, R. Yuste, and K. L. Shepard, Nat. Electron. **2**, 343 (2019).
26) Y. Wang, Y. Zhao, A. Bollas, Y. Wang, and K. F. Au, Nat. Biotechnol. **39**, 1348 (2021).
27) T. Ahmed, S. van den Driesche, J. A. Bafna, M. Oellers, R. Hemmler, K. Gall, R. Wagner, M. Winterhalter, and M. J. Vellekoop, Biomed. Microdevices **22**, 32 (2020).
28) M. Rossi, F. Thei, and M. Tartagni, Sens. Transducers **14**, 185 (2012).
29) M. Crescentini, F. Thei, M. Bennati, S. Saha, M. R. R. de Planque, H. Morgan, and M. Tartagni, IEEE Trans. Biomed. Circuits Syst. **9**, 334 (2015).
30) T. Ahmed, S. van den Driesche, M. Oellers, R. Hemmler, K. Gall, S. P. Bhamidimarri, M. Winterhalter, R. Wagner, and M. J. Vellekoop, Proceedings **2**, 920 (2018).
31) M. Rossi, F. Thei, H. Morgan, and M. Tartagni, Proc. MicroTAS Conf., 2010, p. 1913.
32) R. Miyata, D. Tadaki, D. Yamaura, S. Araki, M. Sato, M. Komiya, T. Ma, H. Yamamoto, M. Niwano, and A. Hirano-Iwata, Micromachines **12**, 98 (2021).
33) A. Hirano-Iwata, Y. Ishinari, M. Yoshida, S. Araki, D. Tadaki, R. Miyata, K. Ishibashi, H. Yamamoto, Y. Kimura, and M. Niwano, Biophys. J. **110**, 2207 (2016).
34) G. Baaken, N. Ankri, A.-K. Schuler, J. Rühe, and J. C. Behrends, ACS Nano **5**, 8080 (2011).
35) G. Baaken, M. Sondermann, C. Schlemmer, J. Rühe, and J. C. Behrends, Lab Chip **8**, 938 (2008).
36) R. Kawano, Y. Tsuji, K. Sato, T. Osaki, K. Kamiya, M. Hirano, T. Ide, N. Miki, and S. Takeuchi, Sci. Rep. **3**, 1995 (2013).
37) K. Kamiya, T. Osaki, K. Nakao, R. Kawano, S. Fujii, N. Misawa, M. Hayakawa, and S. Takeuchi, Sci. Rep. **8**, 17498 (2018).
38) J. L. Poulos, T.-J. Jeon, R. Damoiseaux, E. J. Gillespie, K. A. Bradley, and J. J. Schmidt, Biosens. Bioelectron. **24**, 1806 (2009).
39) B. Lu, G. Kocharyan, and J. J. Schmidt, Biotechnol. J. **9**, 446 (2014).
40) R. Hu, J. Ivica, and M. R. R. de Planque, Ext. Abstr. Solid State Devices and Materials, 2021, p. 413.